

BIOMECHANICAL COMPARISON OF MENISCAL REPAIR SYSTEMS IN SHEAR
LOADING

A Thesis
Submitted to
the Temple University Graduate Board

In Partial Fulfillment
of the Requirements for the Degree
MASTER OF SCIENCE

By
Alan J. Kaufmann
May, 2013

Thesis Approvals:

Kurosh Darvish, Ph.D., Thesis Advisor, Department of Mechanical Engineering
Parasaoran Hutapea, Ph.D., Department of Mechanical Engineering
J. Milo Sowards, MD, Department of Orthopedic Surgery and Sports Medicine

ABSTRACT

A meniscal tear is an injury that often occurs as a result of a varus or valgus rotation of the femur on the tibia coupled with axial rotation while the knee is partially flexed, thus creating preferential loading of the posterior horn and shear forces on the meniscus. Such injuries can be repaired surgically, either with standard suturing techniques or with commercially available all-inside meniscal repair devices, which are designed to make the repair surgery faster, easier, and potentially safer. Many prior biomechanical studies have loaded an excised, repaired meniscus in tension and found that the repaired meniscus performs similarly to an uninjured sample. However, it is more appropriate to apply shear forces to the tissue in order to simulate the mechanism of injury. To date, three prior studies have investigated the biomechanical properties of meniscal repairs in shear, all of which used isolated meniscal tissue samples.

The present study used an *in situ* bovine model to investigate the strength of commercially available meniscal repair systems under a shear loading regime. Medial menisci were torn and subsequently repaired using one of three techniques: standard inside-out vertical mattress sutures, Depuy Mitek Omnispan, or Smith & Nephew Fast-Fix. A control group was left unrepaired. Samples were subjected to a battery of cyclic side loading to create shear forces within the knee.

Statistical analysis (ANOVA) demonstrated no significant difference in the stiffness, shear force, or subsidence between groups. The conclusion that the repair techniques perform similarly is consistent with tensile and *in situ* testing. Pathological observations showed no significant differences between repair devices, but all repaired

samples demonstrated less wear than unrepaired samples, indicating that the experimental model is an effective method for creating wear within the knee. This result indicates that the flexible all-inside devices are mechanically comparable to the more commonly performed conventional suturing techniques. It is concluded that the mechanical performance may not be the best indicator of success of the surgical repair, as long as the device is able to anatomically reduce the tear.

ACKNOWLEDGEMENTS

I would like to acknowledge the assistance of my advisor, Dr. Kurosh Darvish, and my colleagues in the Temple Biomechanics Lab. I would especially like to thank the team from the Department of Orthopedic Surgery at Temple University Medical School, Dr. J. Milo Sowards, Dr. Emeka Nwodin, and Dr. James Lachman, without whom this project would not have been possible.

TABLE OF CONTENTS

	Page
ABSTRACT	i
ACKNOWLEDGEMENT	iii
LIST OF TABLES	v
LIST OF FIGURES	vi
CHAPTER	
1. INTRODUCTION	1
2. MATERIALS AND METHODS	5
3. RESULTS	11
4. DISCUSSION	19
5. CONCLUSION	25
REFERENCES	26
APPENDIX	
A. SOLUTION TO STATIC SYSTEM.....	29

LIST OF TABLES

	Page
TABLE 2.1 – TESTING BATTERY PROTOCOL	8
TABLE 2.2 – WEAR AND FAILURE GRADING CRITERIA	8
TABLE 3.1 – GEOMETRIC MEASUREMENTS.....	12
TABLE 3.2 – SUMMARY OF BIOMECHANICAL CHARACTERISTICS	16
TABLE 3.3 – PATHOLOGICAL RESULTS	17
TABLE 3.4 – SIGNIFICANT DIFFERENCES IN PATHOLOGICAL GROUPS	18

LISTS OF FIGURES

	Page
FIGURE 2.1 – SAMPLE IN TEST APPARATUS	6
FIGURE 2.2 – SPHERICAL CONTACT TO MACHINE ACTUATOR.....	7
FIGURE 2.3 – SAMPLE STIFFNESS DATA	9
FIGURE 2.4 – SAMPLE SUBSIDENCE DATA	10
FIGURE 3.1 – COMPRESSIVE STRESS RESULTS	12
FIGURE 3.2 – SHEAR FORCE RESULTS.....	13
FIGURE 3.3 – SIDE LOAD VS. SHEAR.....	14
FIGURE 3.4 – CUMULATIVE SUBSIDENCE RESULTS.....	15
FIGURE 3.5 – SHEAR STIFFNESS RESULTS	16
FIGURE A.1 – FREE BODY DIAGRAM.....	29
FIGURE A.2 – SHEAR AND MOMENT DIAGRAM.....	31
FIGURE A.3 – FLEXION AND VALGUS ANGLES	32

CHAPTER 1

INTRODUCTION

The meniscus is a semilunar, collagenous soft tissue located both medially and laterally between the femur and tibia within the knee. It functions to increase the contact area between the two incongruent bones, thereby decreasing the stress [1]. The menisci bear approximate 50% of the total compressive load in the joint through the entire range of flexion [2]. The meniscus is primarily anchored at its posterior and anterior horns. When subjected to a force in weight bearing or gait, the meniscus is in compression in the axial direction and tension in the radial direction.

Meniscal tears are a common type of knee injury. Among younger patients, the injury typically occurs as a result of a sports injury, whereas for older patients it is frequently related to degeneration of the meniscus. Tears can occur in a variety of locations, lengths, depths and patterns. Transverse tears, in particular, greatly affect the function of the meniscus as the tissue fibers are primarily oriented longitudinally [3]. Frequently, a meniscal tear results from a varus or valgus rotation of the femur on the tibia, coupled with an axial rotation, while the knee is partially flexed, thus creating preferential loading of the posterior horn and shear forces on the meniscus [4].

Meniscal tears can be treated surgically, depending on the tear pattern and severity. Historically, injured menisci were surgically removed, either partially or completely, though the clinical outcomes were not generally positive due to the loss of the mechanical advantages provided by the tissue. With a better understanding of knee mechanics as well as the rise of arthroscopic procedures, surgical repairs of injured

menisci are becoming more common. There are a variety of suturing techniques available to the treating surgeon. The inside-out technique is commonly believed to be the “gold standard” of repairs. The sutures are placed within the joint capsule and across the meniscal lesion to reduce the tear and then anchored to the exterior of the joint capsule through an additional incision [5]. More recently, commercially available all-inside devices have entered the market. These devices do not require an additional incision to apply and are wholly contained within the joint capsule[6]. Older versions of all-inside devices were rigid, while the newer devices are suture-based with anchors to attach to the meniscal tissue on either side of the lesion [5]. Two examples of all-inside repair devices are the Smith & Nephew Fast-Fix and the Depuy Mitek Omnispan. The Fast-Fix was the first self-adjusting all-inside repair device. It features two flexible anchors (either poly lactic acid or poly-acetal) connected by No. 0 braided polyester suture with a pre-tied sliding-locking knot [5]. The Omnispan features 2 PEEK anchors connected by a loop of No. 0 Orthocord (55% polydioxanone and 45% ultra-high molecular-weight polyethylene) with a pre-tied sliding-locking knot [5]. The ultimate goal of repairing a meniscal tear is to provide the same mechanical properties of an intact meniscus as well as promote healing.

Several studies have been performed to better understand the various surgical methods and products used to repair meniscal tears. Many prior studies loaded excised meniscal tissue in tension. As in normal weight bearing, the compressive forces in the knee displace the meniscus away from the primary anchoring sites, thus creating tensile forces within the meniscus. These studies typically found that the repair systems were

able to withstand similar tensile loads as an intact meniscus in fatigue or load-to-failure scenarios [7-12].

Studies using meniscal tissue *in situ* have also been performed. Becker et al. [13] investigated the distraction forces in repaired bucket-handle meniscal tears in intact human cadaveric knees subjected to compression at various angles of knee flexion. No significant distraction forces in the tear were observed in any loading regimen. Richards et al. [14] used human cadaveric knees with repaired longitudinal meniscal tears and cycled the knees through a full range of motion. They observed that the tear edges were compressed and not distracted and concluded that the ability to reduce the tear anatomically may be more important than load to failure. Staerke et al. [15] simulated weight bearing and gait in intact human cadaveric knees with repaired vertical meniscal tears and found no clinically significant tensile forces on the sutures. These studies all suggest that the primary factor in the mechanical stability of meniscal repairs is not distraction forces and hypothesize that shear forces may be more significant.

The meniscus is typically injured when it is subjected to shear forces, and thus, this loading scenario is of particular biomechanical interest. The effects of shear forces on repairs of excised meniscal tissue have been studied three times to date. Fisher et al. [16] tested three all-inside devices and inside-out horizontal sutures in both axial and shear loading and found that no all-inside device provided the same failure strength as the sutures in either loading regime. Zantrop et al. [17] tested outside-in horizontal and vertical suturing techniques under a shear cyclic loading regime and found that horizontal suturing withstood elongation more effectively, though there was no significant difference in yield or maximum load. Brucker et al. [18] compared several fixation

methods in tensile and shear loading scenarios and found no significant difference in load to failure but did find a difference in mode of failure among flexible repair systems.

The purpose of this study is to biomechanically compare all-inside meniscal repair devices and an inside-out suturing technique in an *in situ* model, as opposed to excised meniscal samples, subjected to a battery of cyclic side loading to create shear forces within the knee.

CHAPTER 2

MATERIALS AND METHODS

This study utilized 32 fresh-frozen bovine hind knees, 8 in each of 4 study groups. Bovine menisci have been shown to have acceptable material properties for use in biomechanical testing [19, 20] and have been used in previous biomechanical studies [12, 18]. Electron microscopy has found that freezing does not affect the collagen structure of the meniscus, and thus does not affect the mechanical properties of the tissue [21].

A peripheral transverse incision was made arthroscopically to create a tear in the medial meniscus while keeping the joint capsule and soft tissues otherwise intact. The tear was then repaired with an inside-out vertical mattress repair with standard sutures, Depuy Mitek Omnispan (Raynham, MA), or Smith & Nephew Fast-Fix (Andover, MA). A fourth group of torn but unrepaired samples was tested as well. All tears and repairs were performed by the same team of orthopedic surgeons according to the manufacturers' guidelines.

Each specimen was potted in aluminum cups using Bondo (3M, Maplewood, MN) with the knee held partially flexed. The tibial end was held completely fixed and unable to rotate, while the femoral end was fixed to a joint. An Interface model 5200 multi axis load cell (Scottsdale, AZ), which measures the thrust and two moments, was mounted horizontally to the tibial support. Each sample was held horizontally with the medial side oriented up in the test setup (Figure 2.1).

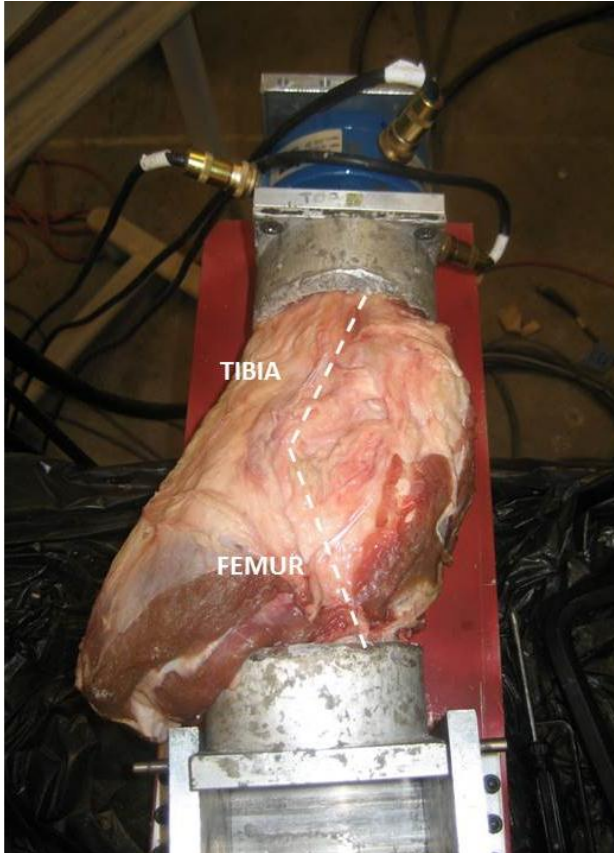


Figure 2.1. Sample in Test Apparatus. The medial side of the sample is shown.

Each specimen was tested on an MTS Landmark 370.10 servo-hydraulic test system (Eden Prairie, MN). A 3/8" diameter steel bolt was inserted into a pre-drilled hole in the medial condyle of the femur, and a curved steel washer was placed underneath a nut to distribute the load over a larger area of the femur. A steel sphere was placed on top of the screw to eliminate any applied moment between the sample and the machine actuator (Figure 2.2).



Figure 2.2. Spherical Contact to Machine Actuator. A 3/8" bolt is inserted into the medial condyle of the femur in line with the actuator and system load cell.

After three cycles of preconditioning, each sample underwent cyclic testing at 2Hz, applying a sinusoidal displacement of 0.25 inches. Four rounds of 2,500 cycles were applied (labeled C1, C2, C3, and C4) for a total of 10,000 cycles (Table 2.1). Between each round of cyclic testing the crosshead and screw positions were readjusted to contact each other, accounting for any subsidence which occurred during testing. No sample catastrophically failed during the cyclic testing. During the cyclic testing, each sample underwent quasi-static testing from 0.05 to 0.25 inches at a rate of 0.01 in/sec to determine the stiffness at three time points: prior to (QS1), halfway through (QS2) and immediately after (QS3). Following the cyclic testing protocol, the repair devices and

meniscal tissue were inspected to determine the amount of wear according to the grading system in Table 2.2. All tests were performed at room temperature.

Table 2.1. Testing Battery Protocol.

Timepoint	Cycles	Rate	Displacement
QS1	3	0.01 in/sec	0.05 in to 0.25 in
C1	2,500	2 Hz	0.05 in to 0.25 in
C2	2,500	2 Hz	0.05 in to 0.25 in
QS2	3	0.01 in/sec	0.05 in to 0.25 in
C3	2,500	2 Hz	0.05 in to 0.25 in
C4	2,500	2 Hz	0.05 in to 0.25 in
QS3	3	0.01 in/sec	0.05 in to 0.25 in

Table 2.2. Wear and Failure Grading Criteria.

Grade	Repair Device Grade	Meniscus Grade
I	Knot slippage	Mild meniscal fraying
II	Fraying around knot	Meniscal fraying and tear lengthening
III	Fraying away from knot	Condral wear
IV	Failure around knot	Tear extending through posterior border
V	Failure away from knot	Plateau or condylar fracture

Force and displacement data were obtained using LabVIEW version 2009 and a SC-2311 DAQ board (National Instruments, Austin, TX). In addition to data recorded by the multi axis load cell, the cross-head displacement and total applied load were measured using the built-in machine transducers with resolutions of 25 μm and 1 N respectively.

Stiffness, magnitude of shear stress, subsidence, and amount of wear were compared between the repair groups. Stiffness was determined by fitting a linear model to the loading portion of the load displacement curve from the quasi-static testing data (Figure 2.3). Shear stress was calculated using the static analysis found in Appendix A. The subsidence in the construct during the cyclic loading was calculating by determining the displacement that occurs in the amount of time that the system load signal plateaus

(Figure 2.4). The amount of wear on the repair device and meniscal tissue is graded based on the rubric in Table 2.1.

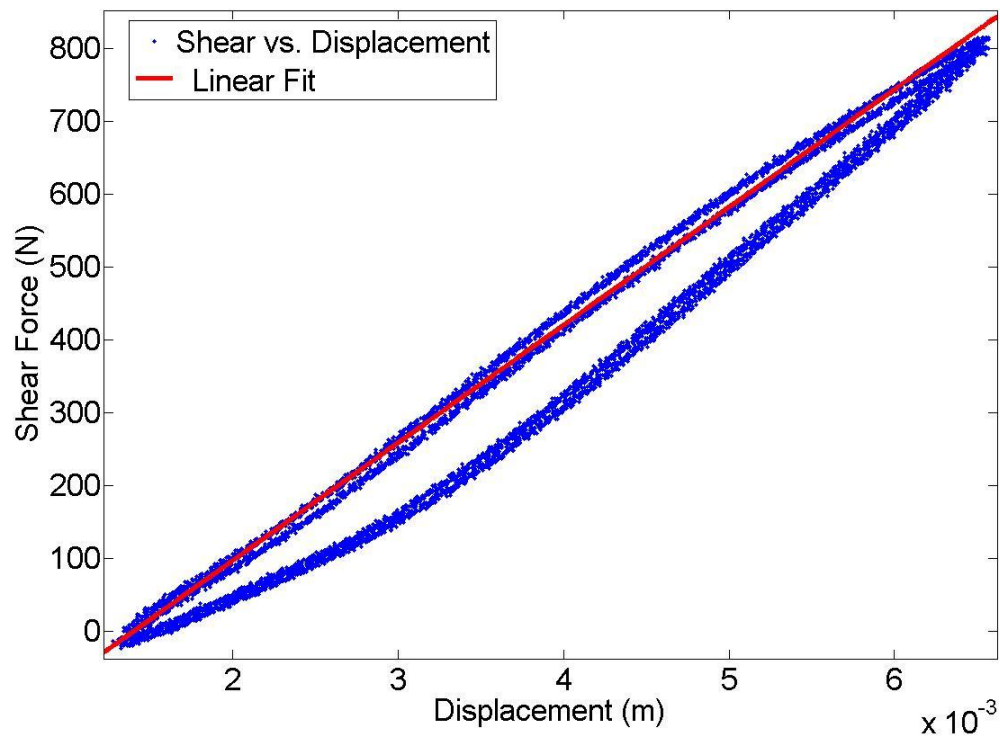


Figure 2.3. Sample Stiffness Data. A linear fit was applied to the loading portion of the load-displacement data from the quasi-static testing.

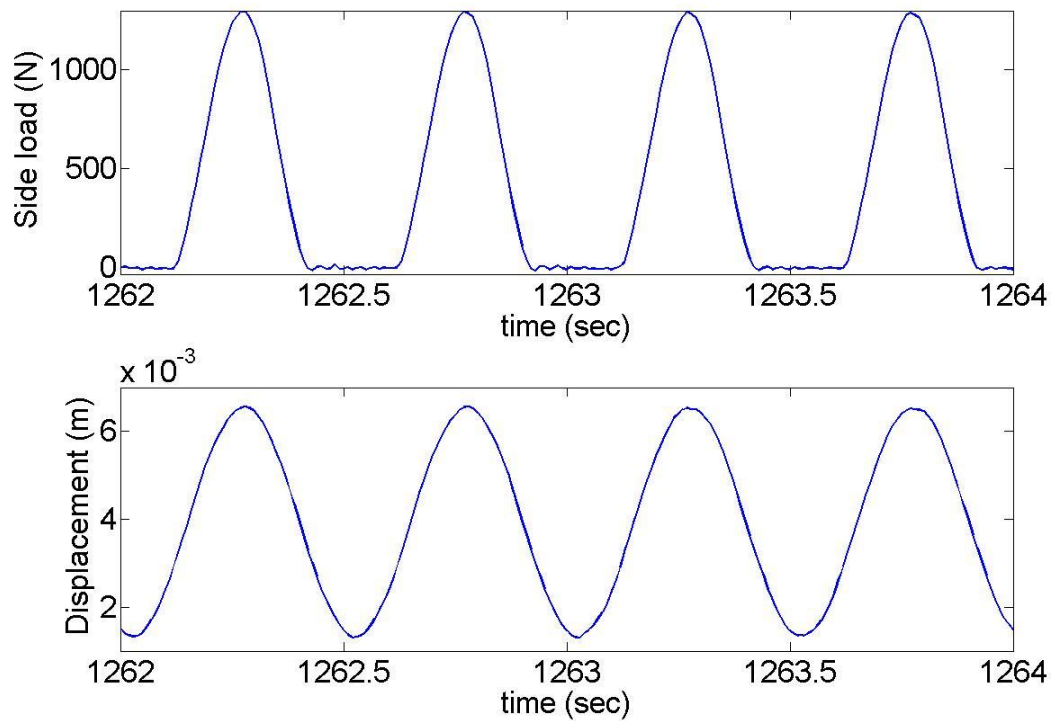


Figure 2.4. Sample Subsidence Data. The subsidence is the amount of displacement that occurs when the load signal plateaus.

Statistical analysis was performed with JMP 8.0.1 software (SAS Institute Inc., Cary, NC) with two sided $p < 0.05$ considered significant. An ANOVA test and was used to compare the four study groups. A matched-pair t-test was used to test for significant changes in mechanical characteristics between rounds of testing. A student's t-test was used to compare the mechanical characteristics between groups of similarly scored repair devices and meniscal tissue samples, as in table 2.1. All values reported represent the mean \pm the standard error of the mean.

CHAPTER 3

RESULTS

Geometric measurements for the four meniscal repair groups are summarized in Table 3.1. No statistically significant differences were found between the four study groups. No geometric measurement was found to linearly correlate with any measured mechanical characteristic. The maximum valgus angle is measured using the sum of the cumulative subsidence after the third round of cyclic testing and the applied displacement. Appendix A contains the trigonometric relations between measured sample lengths and calculated angles.

During the cyclic testing, samples were found to have a compressive stress on the approximate mid-portion of the medial meniscus that was greater than the equivalent of one physiologic bovine standing body weight (40 kPa). No significant difference was found between repair groups at any time point (C1: $p = 0.776$, C2: $p = 0.629$, C3: $p = 0.781$, C4: $p = 0.861$) (Figure 3.1). The compressive stress consistently increased between each round of cyclic testing. Between C2 and C1, the compressive stress increased by 17.1 ± 2.5 kPa ($p < 0.0001$), between C3 and C2, it increased by 8.46 ± 2.03 kPa ($p = 0.0002$), and between C4 and C3, it increased by 4.64 ± 1.74 kPa ($p = 0.0119$).

Table 3.1. Geometric Measurements.

	Vertical Mattress	Omnispan	Fast-Fix	Unrepaired	ANOVA
Femoral Length (mm)	123.64 ± 4.14	112.63 ± 5.07	111.05 ± 6.80	111.68 ± 4.03	$p = 0.3142$
Tibial Length (mm)	83.25 ± 8.43	84.10 ± 5.12	75.51 ± 3.64	75.74 ± 3.83	$p = 0.4141$
Total Length (mm)	202.86 ± 6.05	192.27 ± 5.42	181.59 ± 9.29	182.09 ± 4.48	$p = 0.0942$
Flexion Angle (°)	22.46 ± 2.12	24.64 ± 1.09	26.89 ± 1.07	28.02 ± 0.45	$p = 0.0811$
Maximum Valgus Angle (°)	15.06 ± 1.67	17.37 ± 1.56	15.61 ± 1.76	17.05 ± 1.90	$p = 0.7449$
Area (m ²)	0.023 ± 0.001	0.021 ± 0.001	0.021 ± 0.001	0.023 ± 0.001	$p = 0.2023$
Side	4 Left, 4 Right	5 Left, 3 Right	3 Left, 5 Right	4 Left, 4 Right	

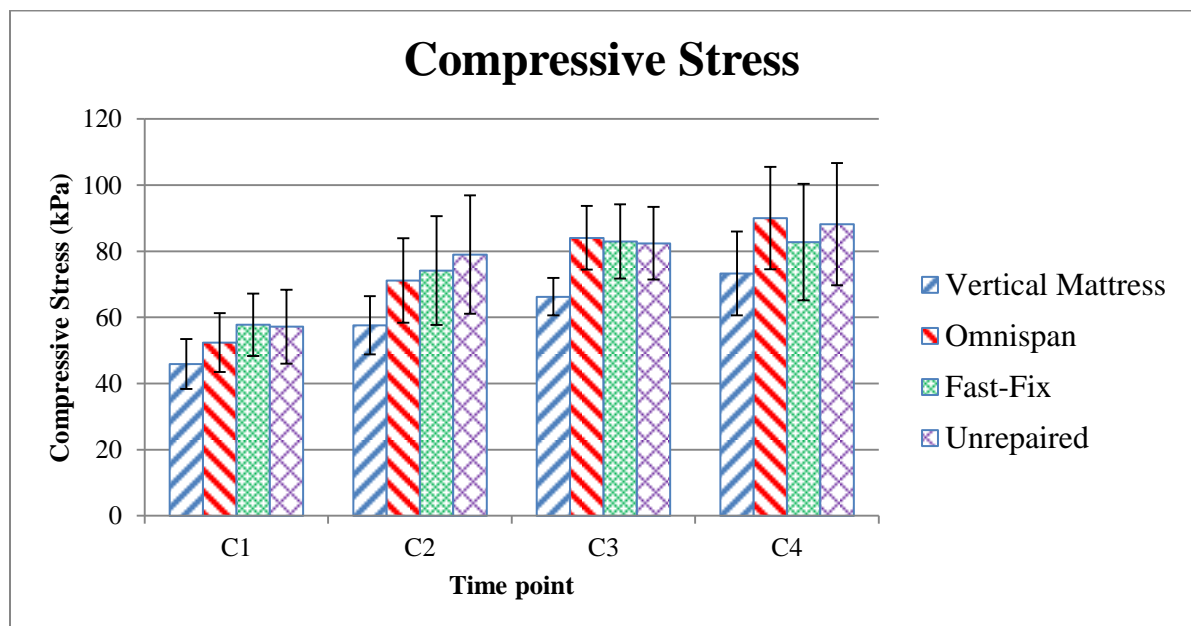


Figure 3.1. Compressive Stress Results.

The magnitude of shear force within the knee was not significantly different between repair device groups (C1: $p = 0.225$, C2: $p = 0.261$, C3: $p = 0.639$, C4: $p = 0.959$) (Figure 3.2). The amount of shear consistently increased between each round of cyclic testing, though the sample exhibited creep behavior during the test. Between C2 and C1, the overall average shear magnitude increased by 122 ± 16 N ($p < 0.0001$), by 59 ± 14 N ($p = 0.0003$) between C3 and C2, and by 31 ± 12 N ($p = 0.0164$). The amount of shear within the knee was found to correlate with the load applied to the medial femoral condyle. The shear force was calculated to be 44.6% of the magnitude of the applied load ($R^2 = 0.9299$), regardless of repair type (Figure 3.3)

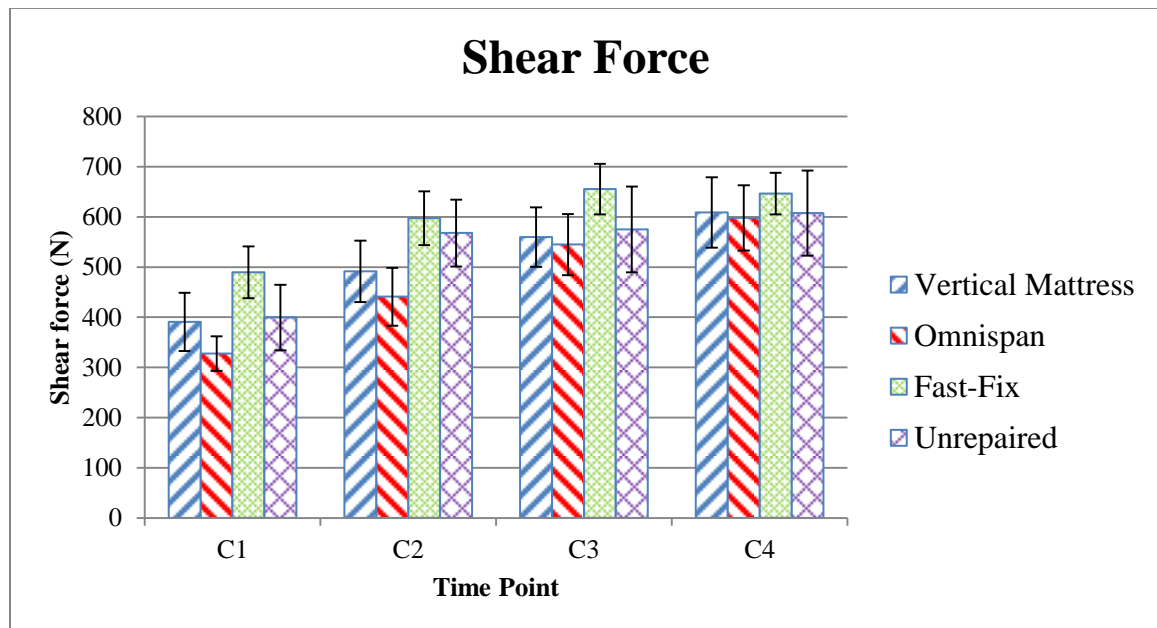


Figure 3.2. Shear Force Results.

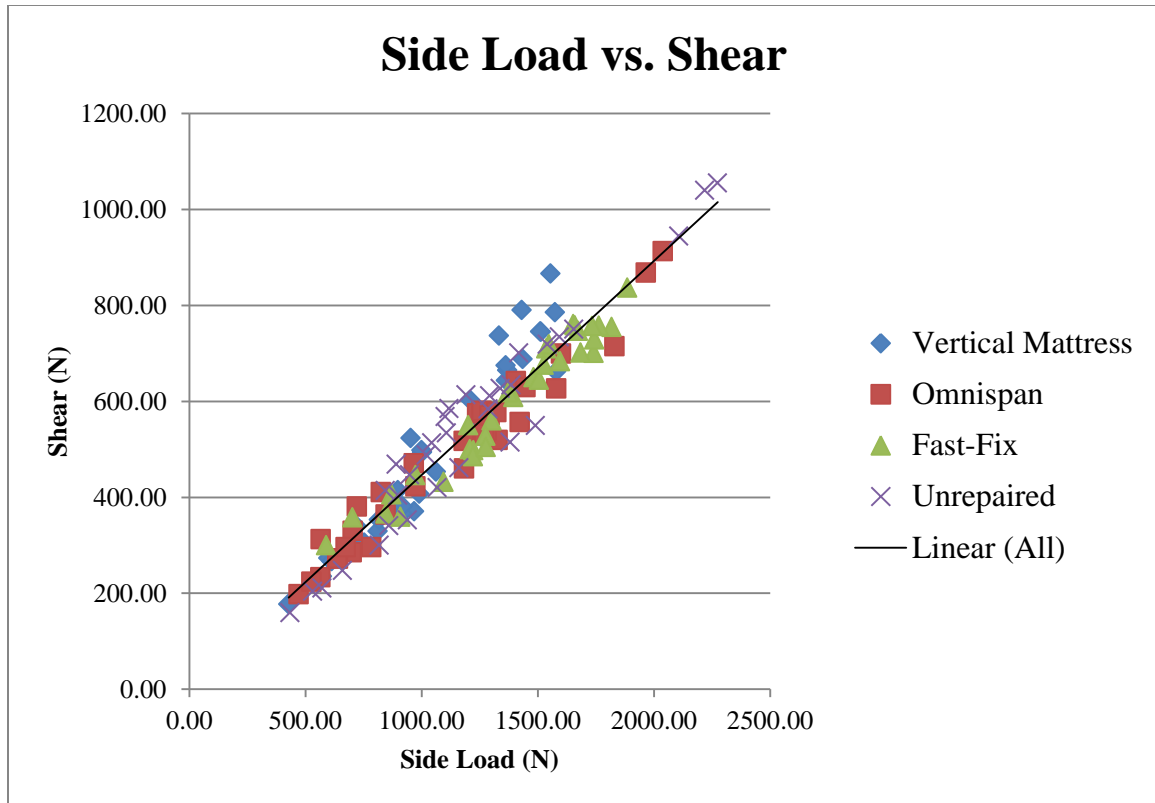


Figure 3.3. Side Load Vs. Shear. The shear force is equal to 44.6% of the applied side load ($R^2 = 0.9299$).

After each round of cyclic testing, the subsidence was measured (Figure 3.4). The subsidence consistently increased throughout the testing protocol, regardless of repair. There were no significant differences found between repair groups at any time point (C1: $p = 0.573$, C2: $p = 0.362$, C3: $p = 0.360$, C4: $p = 0.468$). As some subsidence was observed in each round of testing, the cumulative subsidence must increase by definition. Between C2 and C1, the average subsidence increased by $0.91 \pm .14$ mm ($p < 0.0001$), by 0.63 ± 0.10 mm between C3 and C2 ($p < 0.0001$), and by 0.45 ± 0.09 mm between C4 and C3 ($p < 0.0001$). No displacement was visually observed in the potting material or between the femoral or tibial ends and the potting material.

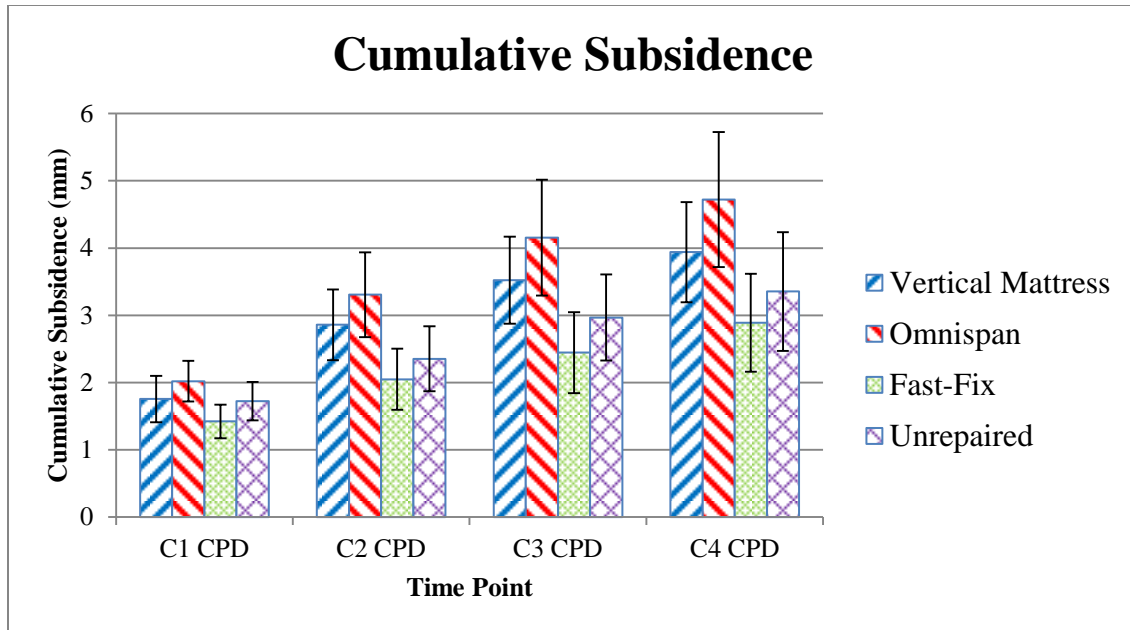


Figure 3.4. Cumulative Subsidence Results.

The shear stiffness was determined in each of the three rounds of quasi-static testing (Figure 3.5). The stiffness was not found to be significantly different between repair groups (QS1: $p = 0.113$, QS2: $p = 0.433$, QS3: $p = 0.300$). The stiffness was found to significantly increase by 54.3 ± 10.5 kN/m between QS2 and QS1 ($p < 0.0001$) but was not a significant increase between QS3 and QS2 ($p = 0.2258$). All of the measured biomechanical characteristics from the battery of testing are summarized in Table 3.2.

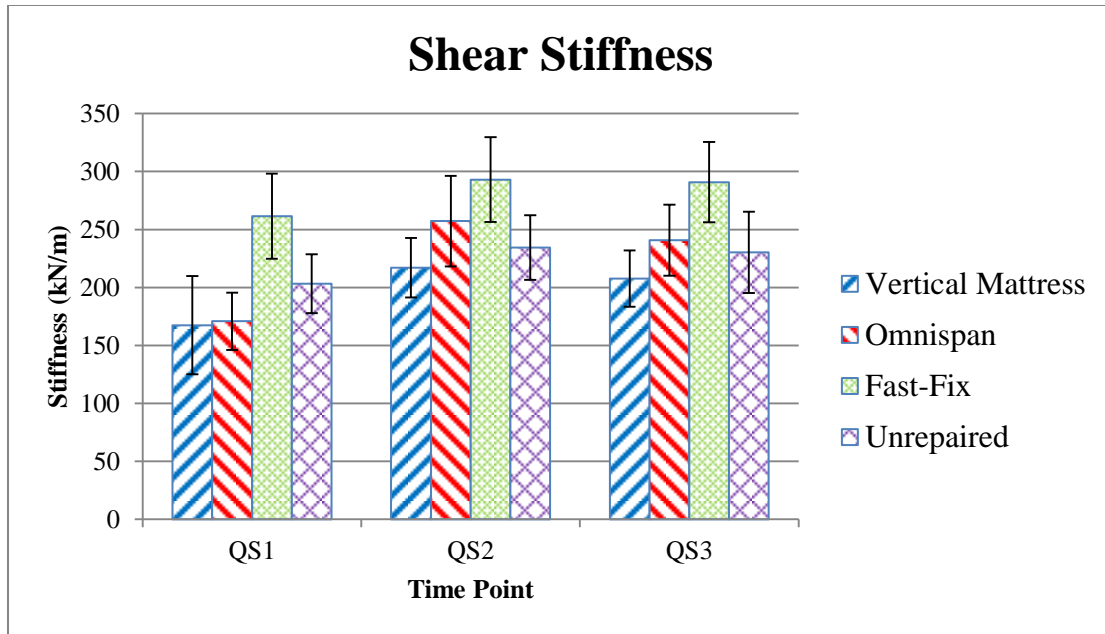


Figure 3.5. Shear Stiffness Results.

Table 3.2. Summary Of Biomechanical Characteristics

		Vertical Mattress	Omnispan	Fast-Fix	Unrepaired	ANOVA
Compressive Stress (kPa)	C1	45.9 ± 7.6	52.4 ± 8.8	57.8 ± 5.6	57.2 ± 12.6	$p = 0.776$
	C2	57.5 ± 8.9	71.1 ± 12.7	74.1 ± 9.7	79.0 ± 15.5	$p = 0.629$
	C3	66.3 ± 9.4	84.1 ± 16.4	83.0 ± 11.2	82.4 ± 17.6	$p = 0.781$
	C4	73.3 ± 11.1	90.0 ± 17.9	82.8 ± 11.0	88.2 ± 18.5	$p = 0.861$
Shear Force (N)	C1	390.7 ± 58.1	327.6 ± 34.6	489.6 ± 51.5	399.4 ± 65.4	$p = 0.225$
	C2	491.6 ± 61.4	440.8 ± 57.9	597.3 ± 53.5	567.7 ± 66.5	$p = 0.261$
	C3	559.6 ± 59.3	544.8 ± 61.0	655.3 ± 50.3	574.9 ± 85.3	$p = 0.639$
	C4	608.6 ± 70.2	598.1 ± 65.2	646.3 ± 41.3	607.3 ± 84.7	$p = 0.959$
Cumulative Subsidence (mm)	C1	1.76 ± 0.34	2.02 ± 0.30	1.42 ± 0.25	1.73 ± 0.29	$p = 0.573$
	C2	2.86 ± 0.53	3.31 ± 0.63	2.05 ± 0.45	2.35 ± 0.48	$p = 0.362$
	C3	3.52 ± 0.65	4.16 ± 0.86	2.45 ± 0.60	2.97 ± 0.64	$p = 0.360$
	C4	3.94 ± 0.74	4.72 ± 1.01	2.89 ± 0.73	3.35 ± 0.88	$p = 0.468$
Shear Stiffness (kN/m)	QS1	74.7 ± 18.9	76.2 ± 11.0	116.6 ± 16.4	90.6 ± 11.3	$p = 0.113$
	QS2	97.0 ± 11.4	114.7 ± 17.5	130.7 ± 16.3	104.5 ± 12.4	$p = 0.433$
	QS3	92.6 ± 10.9	107.3 ± 13.6	129.7 ± 15.4	102.7 ± 15.7	$p = 0.300$

The pathological observations following mechanical testing are found in Table 3.3. No repaired samples received a failure grade higher than 1 for either the repair device or meniscus tissue. Conversely, all of the unrepaired samples displayed significant meniscal fraying (grade 2), and half also exhibited condral wear (grade 3).

There were no significant differences found in any mechanical characteristics between repair devices grades or meniscal tissue grades within repair groups with two exceptions. Within the unrepaired group, there was a significant difference in the compressive stress between samples exhibiting significant meniscal fraying and those also exhibiting condral wear at each time point and a significant difference in the magnitude of the shear force at time point C4 (Table 3.4).

Table 3.3. Pathological Results.

Repair	Number of Samples	Repair Device Grade	Meniscal Tissue Grade
Vertical Mattress	5 samples	0	0
	1 sample	1	0
	1 sample	0	1
	1 sample	1	1
Omnispan	4 samples	0	0
	2 samples	1	0
	2 samples	0	1
Fast-Fix	3 samples	0	0
	2 samples	0	1
	3 samples	1	0
Unrepaired	4 samples	n/a	2
	4 samples	n/a	2 & 3

Table 3.4. Significant Differences In Pathological Groups.

	Unrepaired	Meniscal Tissue Wear Grade		<i>p</i>
		2	2 & 3	
Compressive Stress (kPa)	C1	29.5 ± 11.3	84.8 ± 10.4	0.012
	C2	43.2 ± 10.4	114.7 ± 12.6	0.005
	C3	46.6 ± 11.5	118.2 ± 21.4	0.036
	C4	45.2 ± 12.2	131.2 ± 14.7	0.004
Shear (N)	C4	441.2 ± 83.1	773.4 ± 90.7	0.035

CHAPTER 4

DISCUSSION

This study investigated the differences between inside-out vertical mattress suturing and two all-inside meniscal repair devices, Depuy Mitek Omnispan and Smith & Nephew Fast-Fix, used to repair a peripheral transverse meniscal incision when subjected to cyclic valgus stressing to create shear forces within the knee. Though these repair devices have been previously investigated, no prior study has utilized an *in situ* model in a shear stress loading regime. The loading regime was not designed to simulate normal physiologic loading, as in normal weight bearing or gait, but rather to replicate the mechanism of injury. The loading was applied cyclically both to model the time of a post-operative recovery period and as a worst case scenario to create wear on the tissue and repair device.

No statistically significant difference was found between the four study groups when comparing the stiffness, shear stress, or subsidence at any time point in the battery of mechanical testing. However, there was a difference in the pathological observations made at the conclusion of mechanical testing between the repaired samples, which displayed no more than minor meniscal fraying and knot slippage, and the unrepaired samples, which all displayed significant meniscal fraying and 50% displayed condral wear. The fact that the unrepaired group displayed more wear suggests that the studied repair devices all adequately reduce wear on the meniscal tissue. This also suggests that the experimental testing setup and protocol is an effective model for creating wear within the knee.

The applied loading regime resulted in an axial compressive stress on the approximate mid-portion of the medial meniscus greater than the equivalent of one physiologic bovine standing body weight. Approximately one third of the compressive stress was due to the axial compressive force measured directly by the three axis load cell and two thirds was due to compressive stress in bending. This generated compressive force was due to the fact that the distance between the femoral condyles and tibial plateau is much smaller than the width of the knee, thus when the knee is in valgus rotation the two bones are compressed against each other. This resultant compressive force creates preferential loading of the posterior horn of the medial meniscus. The compressive stress is of particular interest as at least one body weight of compression is typically exerted on the knee in the mechanism of meniscal injury.

The vast majority of prior biomechanical studies on meniscal repairs have been conducted on excised meniscal tissue loaded in tension. Due to the variety of suturing techniques, repair devices, tear patterns and tissue origins, direct comparison proves challenging. Prior studies utilizing either of the two all-inside devices tested in the present study, the Omnispan and the Fast-Fix, are discussed, though no prior study directly compared both. Borden et al. [8] compared the Fast-Fix with vertical mattress sutures in a repair of vertical longitudinal human cadaveric meniscal lesions. The load to failure, stiffness, and displacement were comparable between the devices. The tensile load to failure was 102 ± 11 N for the vertical sutures and 104 ± 31 N for the Fast-Fix samples. Zantop et al. [12] repaired bovine menisci with flexible all-inside devices and conventional suturing techniques and applied a cyclic loading protocol then loaded to failure. The Fast-Fix exhibited significantly higher pullout strength (94.1 N vertical and

80.8 N horizontal) than the horizontal sutures (50.2 N). Chang et al. [9] tested repair devices in peripheral longitudinal porcine menisci lesions under cyclic loading and found the failure load for the vertical sutures (175.6N for #2 FiberWire and 113.8N for #2 Ethibone) to be significantly higher than the Fast-Fix (68.0N). Barber et al. [7] tested the Depuy Mitek Omnispan in a simulated bucket-handle tear in human menisci and found that it did not exhibit a significant difference to inside-out vertical sutures in maximum load. The Omnispan repair group mean load to failure was 88 N. The disagreement between these three prior studies must be due to differences in the experimental designs such as the anchoring of the meniscal tissue to the mechanical testing apparatus. Nevertheless, these studies indicate a general range for tensile load to failure for these repair devices.

Several meniscal repair techniques and devices have been investigated in shear force scenarios in excised meniscal tissues. Fisher et al. [16] compared the tensile and shear load to failure for three all-inside devices and inside-out horizontal sutures in excised porcine mensici. They found that the load to failure in shear was significantly less than that in tension, and that the sutures withstood significantly higher loads than any all-inside device. The horizontal sutures failed at 64.15 ± 17.05 N in shear. In tension, devices failed by suture breakage but in shear the devices failed by pull-out. Zantop et al. [17] investigated the difference between horizontal and vertical suturing in cyclic distraction and shear force scenarios using a porcine model. In distraction, no significant difference was found but in the shear force scenario the horizontal sutures had 1.6 mm less elongation, though no difference in maximum load. Brucker et al [18] tested flexible and rigid all-inside devices, as well as horizontal and vertical sutures, in bovine

lateral menisci in tensile and shear load scenarios. The load to failure was comparable between tensile and shear scenarios, however the stiffness of flexible all-inside repair devices was significantly less than that of other repair devices in shear. They concluded that devices with sufficient stiffness and stability against shear would be favored, especially if the tear is located in the mid-portion of the meniscus.

The three aforementioned shear studies all apply a force perpendicular to the orientation of the sutures or repair device. This loading scenario is a simplification of actual conditions that would occur with the knee. There are a variety of meniscal tear patterns and thus many orientations that the sutures can be placed within the knee. Shear forces in the knee may not necessarily be oriented perpendicular to the direction of the sutures. Each study observed that the tested devices tended to reorient parallel to the tangential force. Furthermore, the meniscal tissue would also be loaded in three dimensions, whereas the excised tissues were held clamped and not loaded physiologically. Thus, *in situ* studies are required to more accurately describe and analyze the biomechanical behavior of meniscal repairs.

While many prior studies have been conducted on excised meniscal tissue from various sources, a small number of studies have been conducted on *in situ* models to better replicate physiologic loading on the meniscal tissue. Becker et al. [13] investigated the distraction forces in a vertical suture repair of bucket-handle tears in the medial menisci of human cadaveric knees. Using a load sensor attached directly to the steel braided wire suture, the distraction forces were measured directly while varying the applied compressive force, knee flexion angle and tibial rotation angle about its long axis. The study measured mean distraction forces up to 4.72 N when under 300 N of axial

compression and up to 2.7 N when free from axial loading, which did not correlate to testing modality. Staerke et al. [15] performed a similar test on human lateral menisci with vertical-longitudinal lesions and measured mean distraction forces up to 4.1 N, regardless of axial compression (either none or 300 N), flexion angle or direction of rotation. Richards et al. [14] came to a similar conclusion after performing a study measuring the compressive and distractive pressures in longitudinal tears throughout the continuous range of knee motion, without applying any compressive force, utilizing both human cadaveric lateral and medial menisci. All three concluded that the displacement forces, as were applied to excised menisci in prior studies, do not occur near the failure point of the sutures or tissue and therefore the assessment of repairs should not be based on the ability to resist such forces. As in the present study, the applied loading parameters did not cause any failure in the repair or meniscal tissue and there were no significant differences in mechanical characteristics. The mechanical characteristics of the repair may not be as important as the ability to anatomically reduce the meniscal tear, which would allow tissue healing to occur.

The current post-operative guidelines for rehabilitation and return to activity following a meniscal repair tend to be conservative. Typically, patients are not permitted to flex the injured knee more than 60° and to weight bear on the leg except in full extension. As the success of the repair appears to be based on the ability to reduce the tear anatomically, and not on mechanical factors, the basis for such guidelines can be evaluated on neuromuscular, rather than mechanical, concerns.

The present biomechanical study does contain limitations. Tissue healing which would naturally occur *in vivo* during the post-operative recovery period is neglected, thus

making the *in situ* model a worst case scenario. A typical knee would be more stable than the tested samples due to the contractions of surrounding muscles, which would occur *in vivo*. Meniscal injuries can also be accompanied by other tissue injuries. For example, the “unhappy triad” consists of meniscal, medial collateral ligament and anterior cruciate ligament tears. It is likely that the mechanical behavior of the sample would be affected by additional injuries to knee. Furthermore, there was a minor amount of desiccation that was observed during the testing process, which could affect the material properties of the tissues.

Further studies are suggested to better understand the repairs of meniscal lesions. A more complex model could be utilized which models the knee as a composite beam composed rigid bones and the soft meniscal and cartilage tissue in three dimensions rather than the two dimensional bending beam model utilized in the present study. The *in situ* experimental test protocol can be used to test a variety of other tear or complex repair configurations, for example bucket-handle tears, meniscal transplants or tissue engineering meniscal scaffolds, which may display different mechanical characteristics. The present results can also be verified using human cadaveric samples for further clinical conclusions. Lastly, clinically correlative studies should be undertaken before extrapolating the results to a patient’s operative or post-operative recovery decisions.

CHAPTER 5

CONCLUSION

The inside-out vertical mattress suturing technique is generally considered to be the “gold standard” in meniscal repairs. However, all-inside repairs have advantages over inside-out or outside-in methods, including simpler instrumentation, reduced operating time and potentially reduced risk of neurovascular injury. Both the Depuy Mitek Omnispan and Smith & Nephew Fast-Fix all-inside meniscal repair devices performed comparably to the inside-out vertical mattress sutures when subjected to an *in situ* shear loading protocol. All repairs adequately prevented wear on the meniscus and further injury. This result, in tandem with the results of other *in situ* meniscal studies, indicates that the flexible all-inside devices are mechanically comparable to the more commonly performed conventional suturing techniques. It is concluded that the mechanical performance may not be the best indicator of success of the surgical repair, as long as the device is able to anatomically reduce the tear.

REFERENCES

- [1] P. Brinckmann, W. Frobin and G. Leivseth. *Musculoskeletal Biomechanics* 2002.
- [2] A. Ahmed. The load-bearing role of the knee menisci. *Knee Meniscus: Basic and Clinical Foundations* pp. 59-73. 1992.
- [3] P. Verdonk and P. Vererfve. Traumatic lesions: Stable knee, ACL knee. *The Meniscus* pp. 45. 2010.
- [4] A. F. Miller RH, *Campbell's Operative Orthopaedics* Anonymous Philadelphia, PA: Mosby, pp. 2395-2600.
- [5] F. A. Barber and E. D. Bava. Meniscal repair: The newest fixators. *Sports Medicine and Arthroscopy Review* 20(2), pp. 95. 2012.
- [6] J. Lozano, C. B. Ma and W. D. Cannon. All-inside meniscus repair: A systematic review. *Clin. Orthop.* 455pp. 134. 2007.
- [7] F. A. Barber, M. Herbert and E. D. Bava. Biomechanical testing of meniscal repair techniques in human cadaveric menisci (SS-30). *Arthroscopy: The Journal of Arthroscopic & Related Surgery* 27(5, Supplement), pp. e46-e47. 2011. . DOI: 10.1016/j.arthro.2011.03.035.
- [8] P. Borden, J. Nyland, D. N. M. Caborn and D. Pienkowski. Biomechanical comparison of the FasT-fix meniscal repair suture system with vertical mattress sutures and meniscus arrows. *Am. J. Sports Med.* 31(3), pp. 374-378. 2003.

- [9] J. H. Chang, H. C. Shen, G. S. Huang, R. Y. Pan, C. F. Wu, C. H. Lee and Q. Chen. A biomechanical comparison of all-inside meniscus repair techniques. *J. Surg. Res.* 155(1), pp. 82-88. 2009.
- [10] V. M. Mehta and M. A. Terry. Cyclic testing of 3 all-inside meniscal repair devices. *Am. J. Sports Med.* 37(12), pp. 2435-2439. 2009.
- [11] C. Rosso, K. Kovtun, W. Dow, B. McKenzie, A. Nazarian, J. P. DeAngelis and A. J. Ramappa. Comparison of all-inside meniscal repair devices with matched inside-out suture repair. *Am. J. Sports Med.* 39(12), pp. 2634-2639. 2011.
- [12] T. Zantop, A. K. Eggers, V. Musahl, A. Weimann and W. Petersen. Cyclic testing of flexible all-inside meniscus suture anchors. *Am. J. Sports Med.* 33(3), pp. 388-394. 2005.
- [13] R. Becker, O. Brettschneider, K. H. Gröbel, R. von Versen and C. Stärke. Distraction forces on repaired bucket-handle lesions in the medial meniscus. *Am. J. Sports Med.* 34(12), pp. 1941-1947. 2006.
- [14] D. P. Richards, F. A. Barber and M. A. Herbert. Meniscal tear biomechanics: Loads across meniscal tears in human cadaveric knees. *Orthopedics* 31(4), pp. 347-350. 2008.
- [15] C. Staerke, O. Brettschneider, K. H. Gröbel and R. Becker. Tensile forces on sutures in the human lateral knee meniscus. *Knee Surgery, Sports Traumatology, Arthroscopy* 17(11), pp. 1354-1359. 2009.

- [16] S. R. Fisher, D. C. Markel, J. D. Koman and T. S. Atkinson. Pull-out and shear failure strengths of arthroscopic meniscal repair systems. *Knee Surgery, Sports Traumatology, Arthroscopy* 10(5), pp. 294-299. 2002.
- [17] T. Zantop, K. Temmig, A. Weimann, A. K. Eggers, M. J. Raschke and W. Petersen. Elongation and structural properties of meniscal repair using suture techniques in distraction and shear force scenarios. *Am. J. Sports Med.* 34(5), pp. 799-805. 2006.
- [18] P. U. Brucker, P. Favre, G. J. Puskas, A. von Campe, D. C. Meyer and P. P. Koch. Tensile and shear loading stability of all-inside meniscal repairs. *Am. J. Sports Med.* 38(9), pp. 1838-1844. 2010.
- [19] C. Proctor, M. Schmidt, R. Whipple, M. Kelly and V. Mow. Material properties of the normal medial bovine meniscus. *Journal of Orthopaedic Research* 7(6), pp. 771-782. 1989.
- [20] M. D. Joshi, J. K. Suh, T. Marui and S. L. Y. Woo. Interspecies variation of compressive biomechanical properties of the meniscus. *J. Biomed. Mater. Res.* 29(7), pp. 823-828. 1995.
- [21] M. Salai, U. Givon, Y. Messer and R. von Versen. Electron microscopic study on the effects of different preservation methods for meniscal cartilage. *Ann. Transplant.* 2(1), pp. 52-54. 1997.

APPENDIX A
STATIC SYSTEM CALCULATIONS

In the experimental setup, the tibial end support (point A) had a vertical and horizontal reaction force and a reaction moment, but the femoral end support (point B) only had a vertical and horizontal reaction force due to the joint in the experimental setup (Figure A.1).

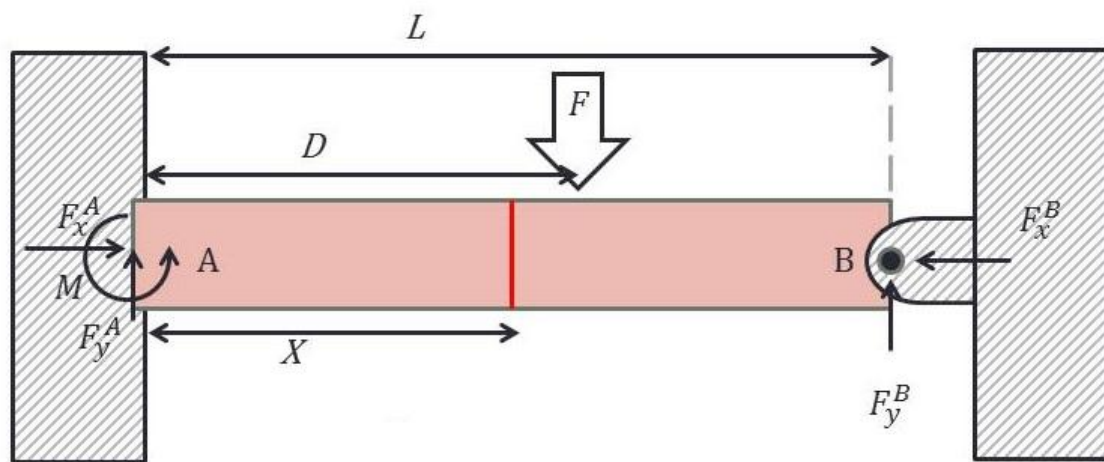


Figure A.1. Free body diagram. Force F is applied by the MTS servo-hydraulic machine actuator; all other forces are reactionary forces. Red line signifies location of menisci at distance X , which is not equal to D .

L represents the total length of the sample. D represents the distance between tibial end and the applied force. d , the height of the load cell, is the distance between the tibial end of the sample and the tibial support. X is the length of the tibia bone. Each length is projected onto the two dimensional plane. Solving this static system simplified to two dimensions yields the following three relations:

$$F_x^A = F_x^B \quad (\text{Equation 1.a})$$

$$F = F_y^A + F_y^B \quad (\text{Equation 1.b})$$

$$M = -F_y^A d - FD + F_y^B L \quad (\text{Equation 1.c})$$

This system would normally be statically indeterminate, as there are five unknown reaction forces and only three equations. However, with the use of the three axis load cell, which measures thrust and two moments, mounted in line with the sample at the tibial support, forces F_x^A and M were measured directly, thus the system becomes solvable.

$$F_x^B = F_x^A \quad (\text{Equation 2.a})$$

$$F_y^B = F - F_y^A \quad (\text{Equation 2.b})$$

$$F_y^A = \frac{F(L - D) - M}{L + d} \quad (\text{Equation 2.c})$$

Once all reaction forces are known, the amount of shear within the knee can be determined (Figure A.2).

The knee flexion angle and the valgus angle can be calculated from the measurements of the lengths of the femoral and tibial components (Figure A.3). L_F and L_T are the lengths of the femoral and tibial components, respectively. L is the total length between the femoral and tibial supports. Therefore, the angle of flexion, θ , is calculated as

$$\theta = 180^\circ - \cos^{-1}\left(\frac{L^2 - L_T^2 - L_F^2}{-2L_T L_F}\right) \quad (\text{Equation 3})$$

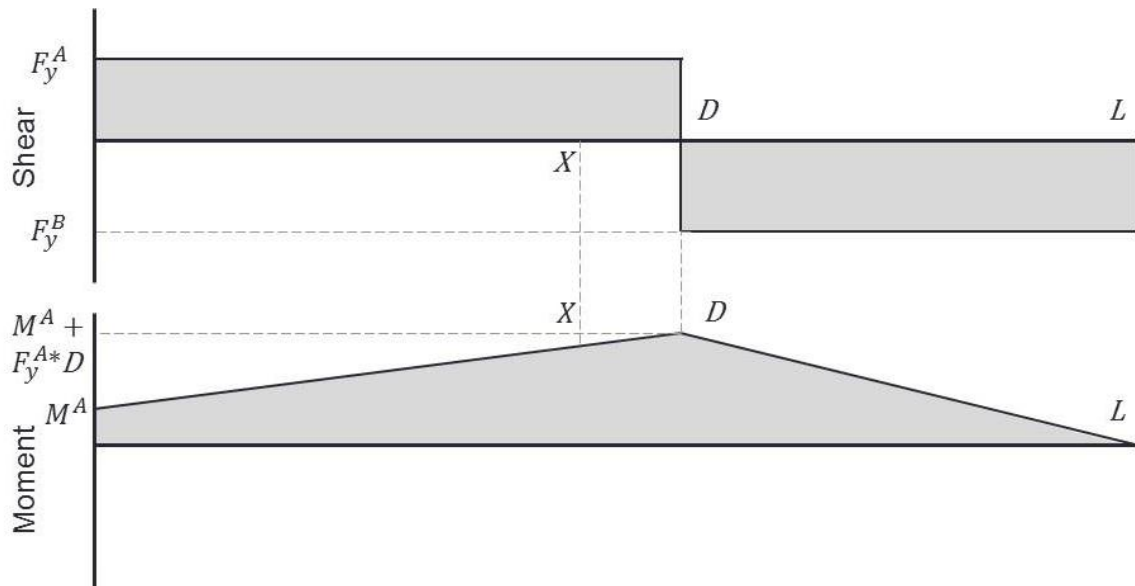


Figure A.2. Shear and Moment Diagram.

L_S is the distance between the femoral support and the site of the steel screw, which is inserted in the medial femoral condyle and serves as the point of contact with the machine actuator. Therefore, the valgus angle, ϕ , can be calculated as

$$\phi = 180^\circ - \sin^{-1}\left(\frac{L_D}{L_S}\right) - \sin^{-1}\left(\frac{ZL_F}{L_S L_T}\right) \quad (\text{Equation 4})$$

where Z is the applied displacement. As the displacement is applied, the projected lengths would become longer, thereby creating the axial compression, though this change is neglected in the trigonometric relations and in the static analysis.

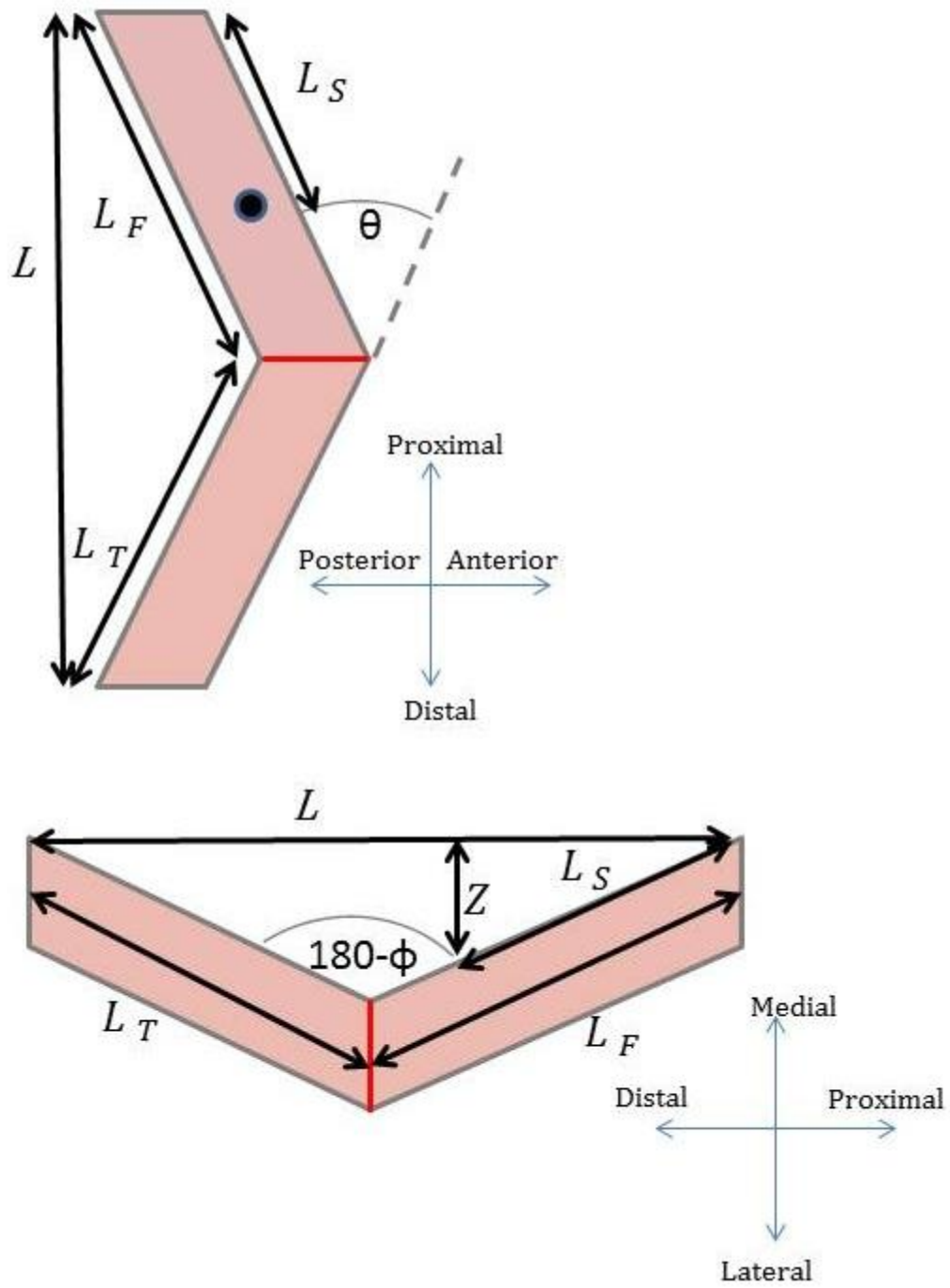


Figure A.3. Flexion and Valgus Angles.